

Climate Change, Sea Level Rise, and Flooding in the Lower Snohomish River Basin

Guillaume Mauger and Se-Yeun Lee
Climate Impacts Group, University of Washington

December 10, 2014



Table of Contents

INTRODUCTION	3
APPROACH.....	4
HYDRAULIC MODELING.....	4
UPSTREAM BOUNDARY CONDITIONS	7
<i>Climate Projections</i>	<i>7</i>
<i>Streamflow Simulations</i>	<i>8</i>
<i>Extreme flood events.....</i>	<i>8</i>
<i>Flood Hydrographs.....</i>	<i>12</i>
LOWER BOUNDARY CONDITION.....	16
<i>Tides and Surge</i>	<i>16</i>
<i>Sea Level Rise</i>	<i>17</i>
<i>Vertical Land Motion.....</i>	<i>17</i>
<i>Model runs</i>	<i>18</i>
RESULTS.....	19
ACKNOWLEDGEMENTS	22
REFERENCES.....	25

Introduction

Over the past decade, numerous climate change assessments have estimated changes in river flooding, sea level rise, and storm surge. Few, however, have quantified the joint impacts of both on future changes in flood risk. The lower mainstem of the Snohomish River is impacted from the marine side by storm surge and sea level rise (SLR), and from the freshwater side by seasonal changes in river flow and hydrologic extremes. We assessed the impacts of climate change on sea-level rise, storm surge and peak streamflows in the lower Snohomish River, located in the Puget Sound Region of Washington State (Figure 1). Building on previous work in the Skagit River basin (Hamman et al., 2014; Hamman, 2012), we developed projections of changing inundation in the lower Snohomish. Results from this work have been incorporated into a decision support tool developed by The Nature Conservancy (TNC), designed to support multi-objective floodplain management by partners across Puget Sound.

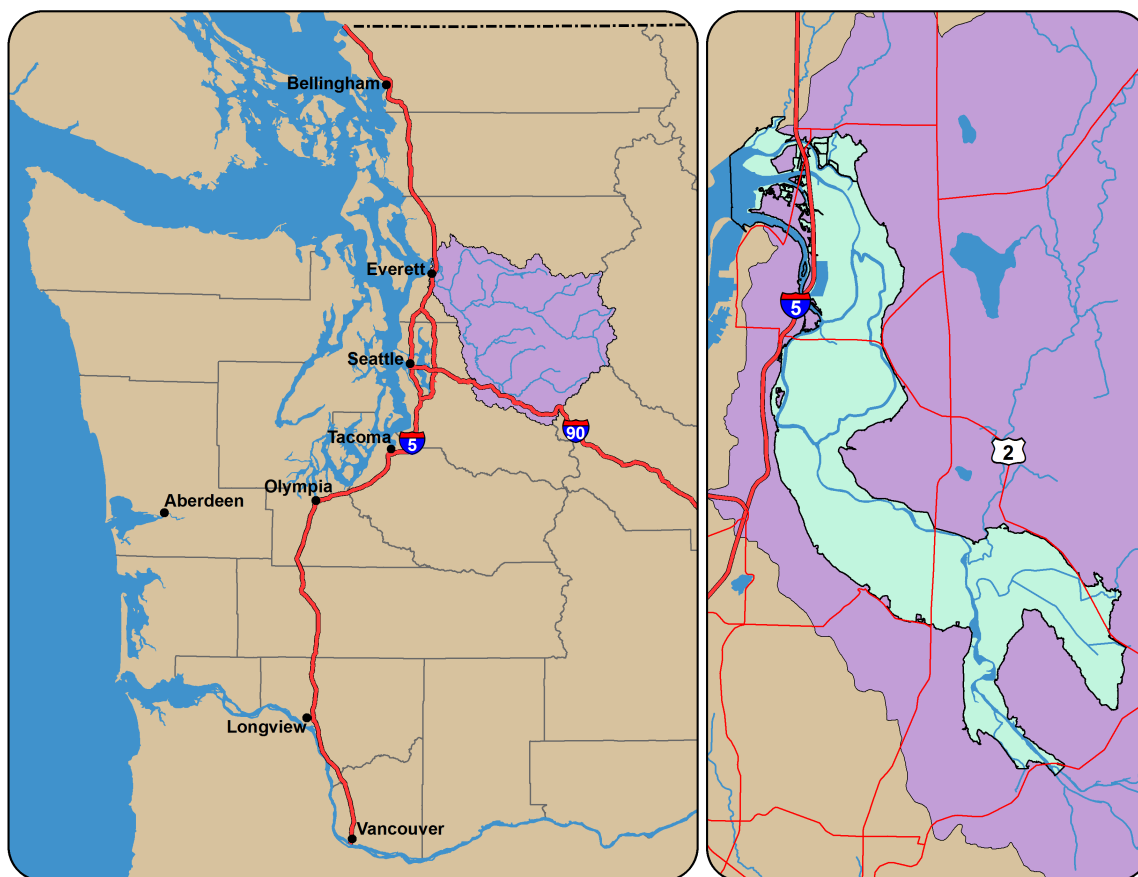


Figure 1 – Study domain. On the left is a map showing the entire Snohomish River basin, which extends from the crest of the Cascade mountains to Puget Sound. On the right is a close-up of the study domain – extending from Puget Sound to the town of Monroe.

Approach

To assess the impact of climate change on flood inundation in the lower Snohomish River, we coordinated with WEST Consultants, who finalized the development of an unsteady-flow hydraulic model for the lower Snohomish River. CIG developed projections of changing storm surge, SLR, and riverine flooding. These provided boundary conditions for the hydraulic model, which was used to estimate the combined effects of sea level rise and changing peak flows on flood inundation.

Hydraulic Modeling

WEST Consultants had developed a one-dimensional unsteady-flow model of the Snohomish River for a FEMA flood insurance re-study using a U.S. Army Corps of Engineers (USACE) model called UNET (Unsteady NETwork Model; WEST, 2001). Since about 2010, WEST had been steadily converting this model to a more modern program, also developed by USACE – called the Hydrologic Engineering Center’s River Analysis System (HEC-RAS) – as opportunities arose during several projects. These included the Everett River study (WEST, 2012) and the Smith Island study (WEST, 2011), and used the latest LiDAR overbank and in-water bathymetric surveys to redefine cross sections and add more resolution in project areas. During this study, WEST completed the model conversion by adding the storage areas and levees, and by re-aligning the cross sections and their numbering to conform to FEMA’s river mile shape file. The update model was calibrated to data from three streamflow gauges collected during water year 2009. For this study, we used HEC-RAS version 4.1.0.

HEC-RAS is a suite of programs that includes one-dimensional (1D) unsteady flow. The unsteady-flow module solves the one-dimensional St. Venant equations (conservation of mass, and conservation of momentum) in a one-dimensional network of reaches, storage areas, and lateral structures (Figure 2). The one-dimensional reaches represent the main stem of the Snohomish River from Monroe to Puget Sound, various parts of the distributary system, including Ebey, Steamboat, Union Sloughs, and the Marshlands Diking District area on the left overbank opposite the City of Snohomish. Storage areas, simulating only conservation of mass, represent “ponding” areas such as the French Slough Diking District and various areas between the leveed sloughs in the downstream distributary area. We used lateral structures to simulate the levees that separate the reaches from the storage areas or separate adjacent storage areas.

We specified time-varying water surface elevations at the limits of the downstream reaches to represent tides in Puget Sound. At the upstream extent of the Snohomish River, we specified hourly river flows from the USGS streamflow gauge at Monroe. Near the City of Snohomish, we specified lateral inflows from the Pilchuck River using data from the most-downstream USGS streamflow gauge on the Pilchuck River. HEC-RAS then simulates water levels and velocities in the various reaches, and water levels in the various storage areas. By adjusting the boundary conditions the HEC-RAS model can be used to simulate potential inundation due to projected sea level rise, storm surge and floods (Figure 3).

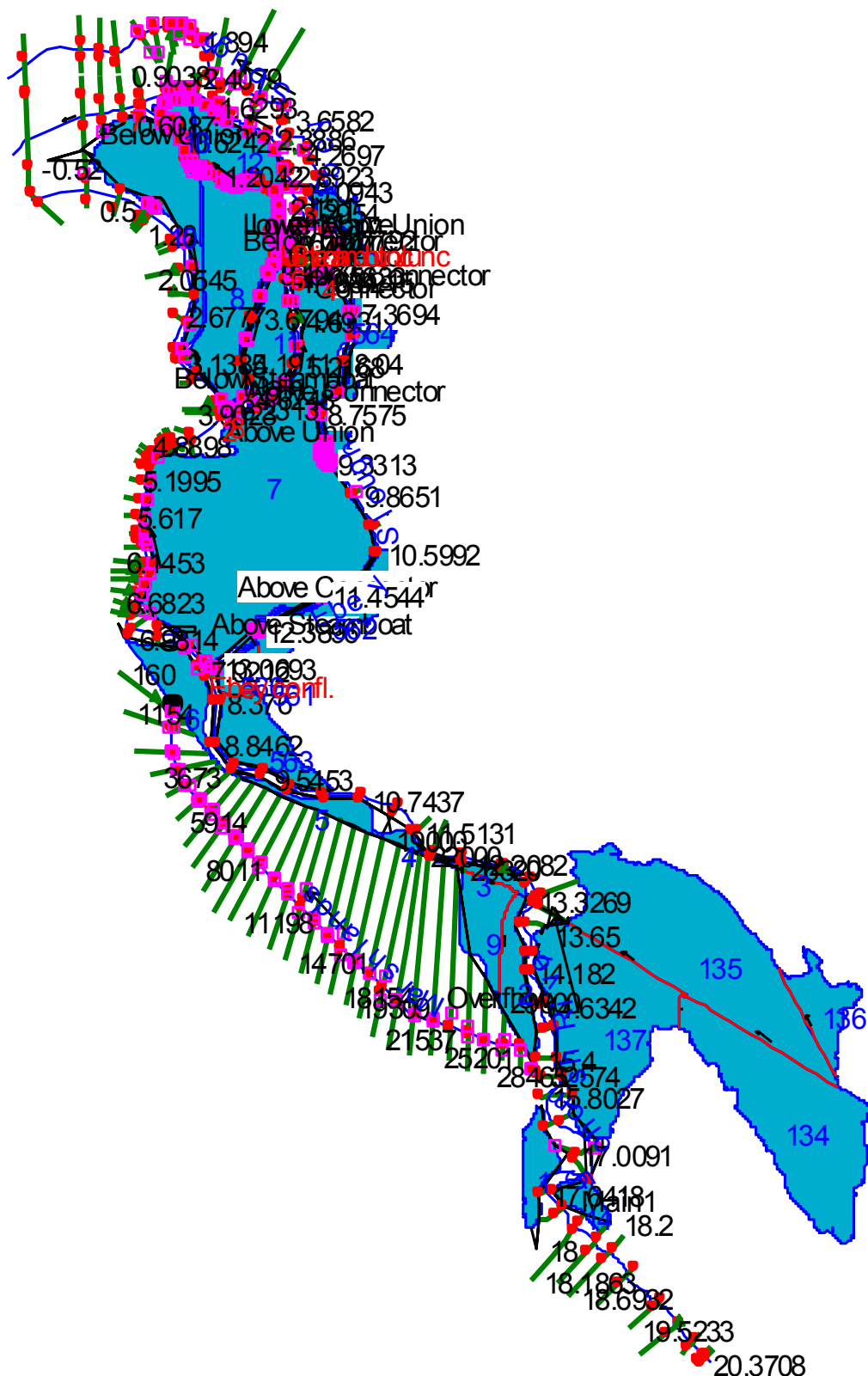


Figure 2 – Schematic of the one-dimensional layout of the HEC-RAS 1D model of the lower Snohomish River system.

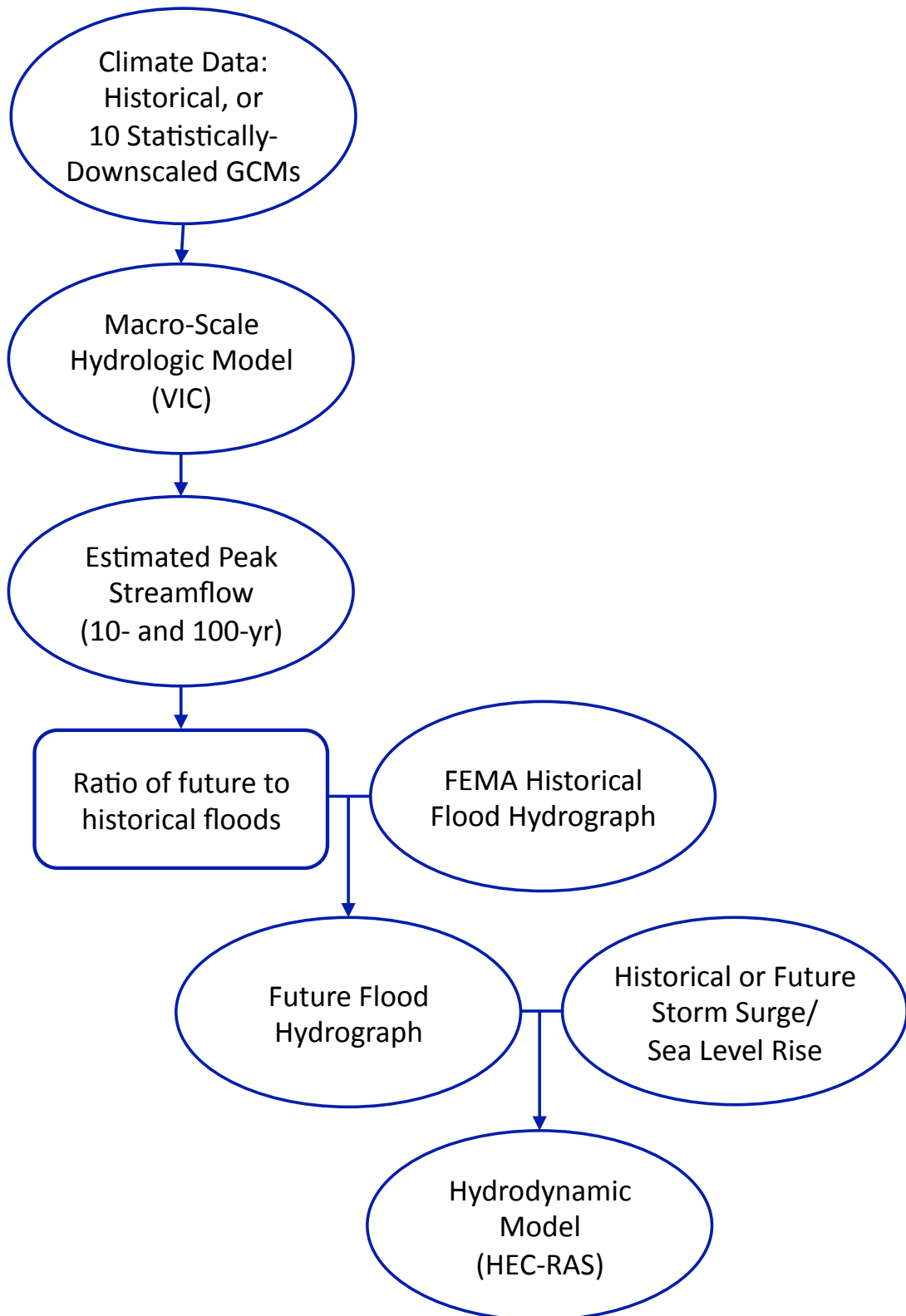


Figure 3 – Flow diagram illustrating the chain of numerical models used for this project.

Upstream Boundary Conditions

As an upstream boundary condition to the HEC-RAS model, we used existing historical hydrographs at different return periods that were developed for a Flood Insurance Study for Federal Emergency Management Agency (FEMA) Region 10 (WEST, 2001). We then developed projected future flows by scaling historical hydrographs. The scaling factors were determined using the ratio of future to historical flood events at different return periods, obtained from hydrologic simulations.

Climate Projections

For climate data projections, we used the existing downscaled hydro-climatic projections from Hamlet et al. (2013). These were produced using global climate model (GCM) projections from the Coupled Model Inter-comparison Project phase 3 (CMIP3; Meehl et al., 2005). The 10 GCMs with the highest fidelity to Pacific Northwest climate were downscaled using the statistically-based Hybrid Delta (HD) approach (Hamlet et al. 2013). The method works by perturbing the observed historical record using the changes in the probability distribution – in monthly temperature and precipitation – simulated by each GCM. Projections were obtained for the A1b greenhouse gas scenario (which assumes moderate 21st century emissions; Nakicenovic et al., 2000), for two future 30-year time periods; the 2040s (2030-2059) and the 2080s (2070-2099), relative to 1970-1999. The HD approach was applied individually to each of the ten GCM scenarios in order to estimate the uncertainty in streamflow statistics deriving from uncertainties in temperature and precipitation projections from different GCMs.

Statistically-downscaled projections use an empirical relationship between local and large-scale weather patterns to estimate variations in climate at finer scales. Implicit in such approaches is the assumption that there is a unique functional relationship between large-scale and local-scale variations. Although statistical approaches have been shown to perform well in many situations (e.g.: Abatzoglou et al., 2013), they are limited by the range of conditions sampled in the historical record, and cannot capture novel processes or non-linear responses to anomalous warming. For example, a recent study – using a regional climate model simulation over the Pacific Northwest (Salathé et al., 2014) – showed that projected changes in heavy precipitation could have a substantial impact on future flood risk in warm coastal river basins. This result differs from previous studies (e.g.: Tohver et al., 2014), which emphasized the vulnerability of cooler basins as a result of the loss of snowpack. This highlights the need to consider multiple approaches to projecting changes in flood risk.

To assess the impact of downscaling approach on streamflow projections, we included one dynamically downscaled scenario in the analysis. Dynamical downscaling is performed by running a regional climate model with boundary conditions taken from a global model. In this case, the Weather Research and Forecasting (WRF) regional model was run using boundary conditions from the ECHAM5 global model (Roeckner et al., 1999; 2003) and SRES A1b emissions scenario. The WRF simulations were implemented over the northwest United States at a grid spacing of 12 km (see Salathé et al., 2010 and Salathé et al., 2014 for details).

In all cases, the results of the dynamically-downscaled projections were found to be within the range of the 10 statistically-downscaled projections. Unfortunately, only one dynamically-downscaled hydrologic projection is currently available, and it was far beyond the scope of the current project to produce additional simulations. However, the agreement between the WRF and HD projections does suggest that the results are not unduly affected by the choice of downscaling approach.

Streamflow Simulations

To produce the upstream boundary conditions for HEC-RAS – streamflow at the Pilchuck River and the Snohomish River near Monroe – we used the physically-based, distributed, Variable Infiltration Capacity (VIC) macroscale hydrologic model (Liang et al., 1994; Gao et al., 2010), implemented at 0.0625-degree resolution (~5 km x 7 km per grid cell; Elsner et al., 2010; Hamlet et al., 2013). Using daily minimum and maximum temperature, precipitation, and winds, the VIC model simulates water and energy balance variables such as snowpack, soil moisture, evapotranspiration, runoff, and baseflow. The historical baseline simulations cover 91 water years (October to September) for 1916-2006 (Elsner et al. 2010). Since the downscaling approach works by perturbing the observed historical record, future simulations cover the same 91 year period, with temperature and precipitation adjusted to reflect the global model projections (see above).

As a post-processing step, daily runoff and baseflow were routed to produce daily streamflows at the Pilchuck River and the Snohomish River near Monroe. This is an off-line calculation, based on a routing model developed by Lohmann et al. (1996), that takes a pre-determined routing network (based on a Digital Elevation Model, or DEM) and aggregates runoff from individual model grid cells into the stream channel network.

The VIC hydrologic model generally captures many important features of hydrologic variability but the model output can be biased in comparison with naturalized or observed streamflows. To remove these biases a quantile mapping procedure was used, in which the probability distribution of simulated monthly flow is scaled to match the distribution of observed monthly streamflow (Snover et al. 2003; Vano et al., 2010). Observed flows were obtained from the two U.S. Geological Survey (USGS) streamflow gauges listed in Table 1.

Table 1 – USGS streamflow gauges used to bias-correct model-simulated streamflow.

<i>Station Name</i>	<i>USGS ID #</i>	<i>Length of Obs. Record</i>
Pilchuck River near Snohomish, WA	12155300	WY 1993-2006
Snohomish River near Monroe, WA	12150800	WY 1964-2006

Extreme flood events

For flood statistics, we extracted the 1-, 3-, 5-, and 7-day consecutive highest flows for each water year and ranked the values by flow magnitude. A quantile was assigned to each value

using an unbiased quantile estimator (Stedinger et al. 1993). These were fit to a Generalized Extreme Value (GEV) Distribution using L-moments (Wang 1997; Hosking and Wallis 1993; Hosking 1990). For historical as well as two future time periods, we estimated flood magnitudes with 10-year (Q10), 50-year (Q50) and 100-year (Q100) return frequencies from the fitted GEV distributions. These are defined based on the probability that peak flows exceed a certain threshold on any given year. Sometimes referred to as the “Annual Chance of Exceedance” (ACE), the 3 return frequencies correspond to an ACE of 10%, 2%, and 1%, respectively.

The ratios of future to historical flood events at a given return interval were used to scale observationally-based hydrographs of historical extreme flows. Figures 4 and 5 show the ratios of future to historical floods for all ten scenarios for both the Snohomish and the Pilchuck Rivers. The corresponding maximum, median and minimum change projected by all ten GCMs is listed in Tables 2 and 3. Note that there is some tendency towards larger changes for the longer period flows (e.g.: 7-day relative to 1-day), especially for the 50- and 100-year events, although the differences are small compared to the range among models.

Table 2 – Ratio of future to historical floods for the Snohomish River for 1-day, 3-day, 5-day and 7-day consecutive highest flows with a return frequency of 10-year (Q10), 50-year (Q50) and 100-year (Q100) for the 2040s and 2080s. These correspond to the 10%, 2%, and 1% ACE, respectively.

Time Periods	Return interval	Ratio of future to historical peak flow			
			1-Day	3-Day	5-Day
2040s	Q10 (10% ACE)	Max	1.60	1.61	1.65
		Mean	1.25	1.27	1.29
		Min	1.06	1.08	1.09
	Q50 (2% ACE)	Max	1.49	1.47	1.51
		Mean	1.15	1.17	1.20
		Min	1.01	1.03	1.04
	Q100 (1% ACE)	Max	1.44	1.41	1.45
		Mean	1.10	1.12	1.16
		Min	0.96	0.97	1.03
2080s	Q10 (10% ACE)	Max	1.78	1.79	1.83
		Mean	1.40	1.42	1.43
		Min	1.16	1.18	1.20
	Q50 (2% ACE)	Max	1.64	1.63	1.64
		Mean	1.27	1.30	1.31
		Min	1.04	1.08	1.10
	Q100 (1% ACE)	Max	1.57	1.56	1.56
		Mean	1.22	1.25	1.26
		Min	0.98	1.04	1.06

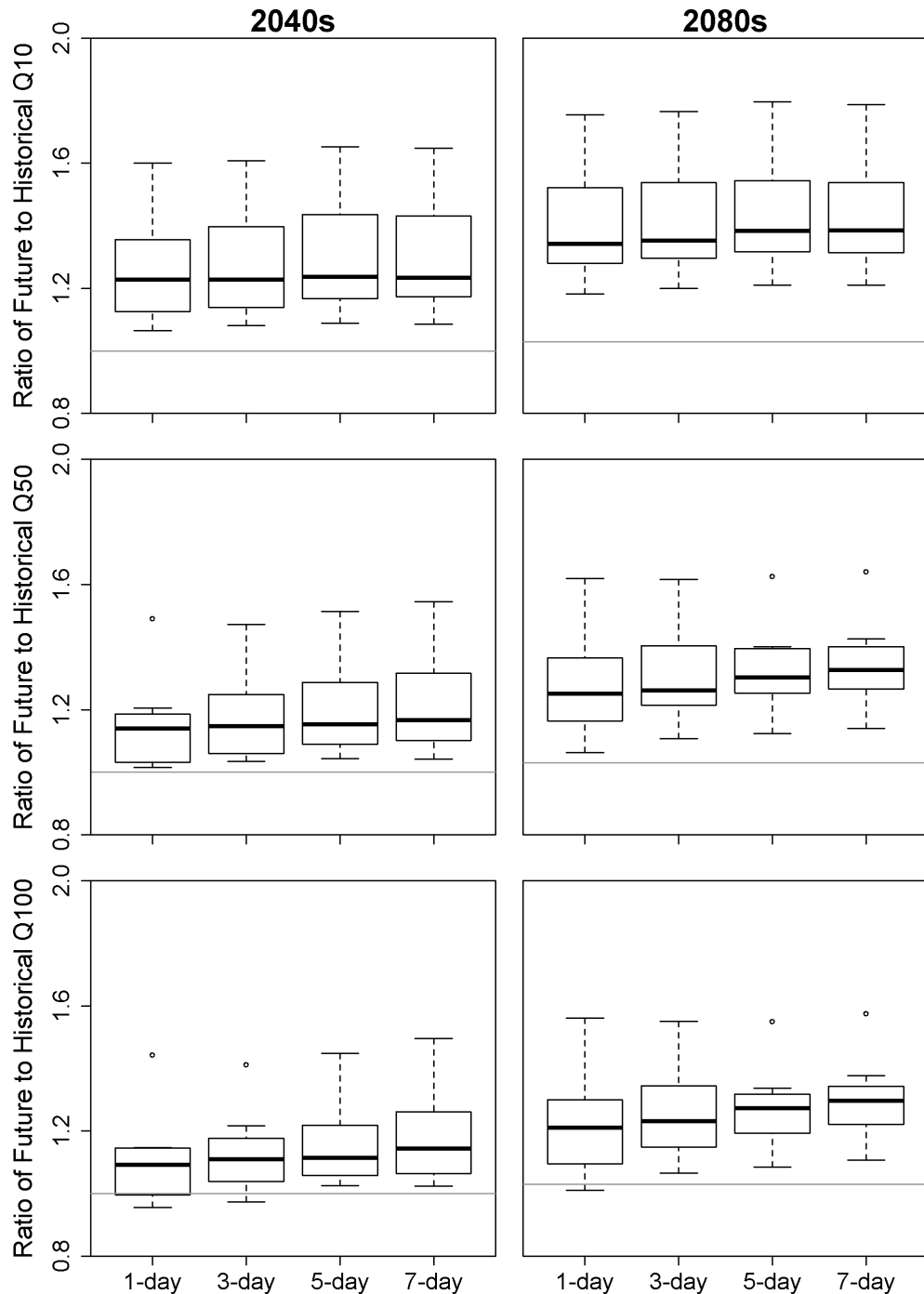


Figure 4 – Ratio of future to historical peak streamflow events for the Snohomish River at Monroe. Box plots of the ratios are shown for 1-day, 3-day, 5-day and 7-day consecutive peak flows with a 10-year (Q10, top), 50-year (Q50, middle) and 100-year (Q100, bottom) return frequency for the 2040s (left panels) and 2080s (right panels). These correspond to the 10%, 2%, and 1% ACE, respectively. Boxes show the median, 25th, and 75th percentile values among all projections, whiskers denote the minimum and maximum values unless the distance from the minimum to the first quartile value is greater than 1.5 times the interquartile range, in which case the whisker denotes 1.5 times the interquartile range and outliers are shown as open circles. The line of zero change is shown in grey.

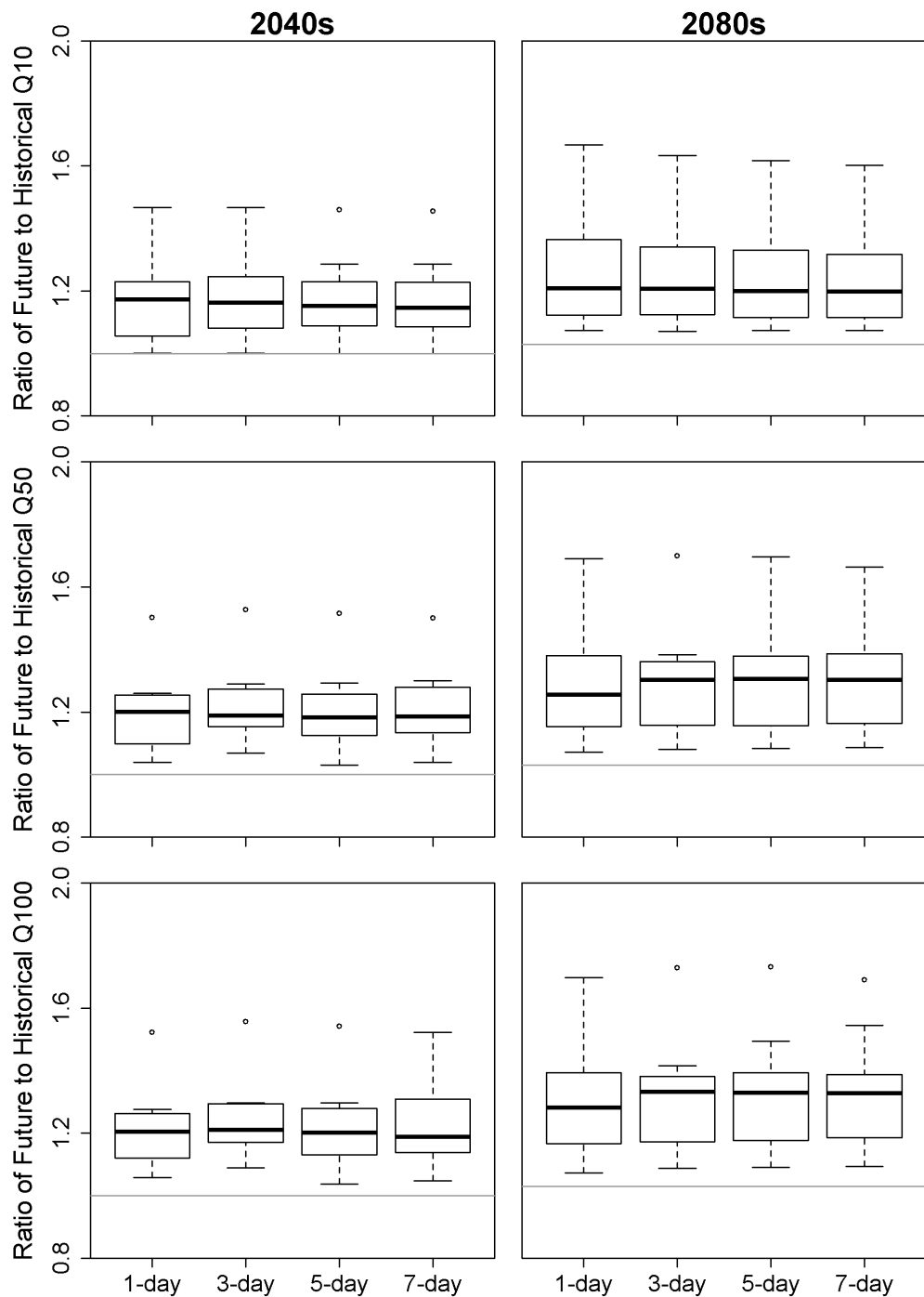


Figure 5 – As in Figure 4 but for the Pilchuck River.

Table 3 – As in Table 2 but for the Pilchuck River.

Time Periods	Return interval	The ratio of future to historical peak flow				
			1-Day	3-Day	5-Day	7-Day
2040s	Q10 (10% ACE)	Max	1.47	1.47	1.46	1.45
		Mean	1.17	1.18	1.17	1.17
		Min	1.00	1.00	1.00	1.00
	Q50 (2% ACE)	Max	1.50	1.53	1.52	1.50
		Mean	1.20	1.22	1.20	1.21
		Min	1.04	1.07	1.03	1.04
	Q100 (1% ACE)	Max	1.52	1.56	1.54	1.52
		Mean	1.21	1.24	1.22	1.23
		Min	1.06	1.09	1.04	1.05
2080s	Q10 (10% ACE)	Max	1.69	1.65	1.63	1.62
		Mean	1.25	1.25	1.24	1.24
		Min	1.05	1.05	1.05	1.05
	Q50 (2% ACE)	Max	1.71	1.72	1.72	1.68
		Mean	1.27	1.29	1.29	1.29
		Min	1.05	1.06	1.06	1.06
	Q100 (1% ACE)	Max	1.72	1.75	1.76	1.71
		Mean	1.29	1.32	1.33	1.33
		Min	1.05	1.06	1.07	1.07

Flood Hydrographs

WEST Consultants developed synthetic hydrographs for the 10-, 50-, 100- and 500-return intervals for two river locations, as a part of a Flood Insurance Study for Federal Emergency Management Agency Region 10 (FEMA; WEST, 2001). For the Snohomish River, WEST used the “balanced hydrograph” approach, in which a hydrograph is constructed to be consistent with the observed exceedance probabilities of instantaneous, 1-, 3-, 5-, and 7-day peak flows, and skewed to match the relative duration of the rising and receding limbs of observed flood hydrographs. For the Pilchuck River, which contributes less than 10% of the Snohomish River flow volume, WEST used an observed hydrograph obtained from the U.S. Army Corps of Engineers (USACE), and simply scaled the peak to match the estimated peak flows for each return interval. As a conservative estimate of flood risk, peak flows for the Pilchuck and Snohomish Rivers were assumed to occur at the same time. Tables 4 and 5 list the time series of the historical FEMA hydrographs developed by WEST consultants.

In order to simplify the analysis and constrain the scope of the project, we omitted the 50-year floods and considered only the 10- and 100-year flood events in the present analysis. Based on consultation with WEST and The Nature Conservancy, these were deemed most relevant to floodplain management. We used the synthetic 10- and 100-year historical flood hydrographs developed by WEST as baseline upstream boundary conditions and developed future flood

Table 4 – Time series of historical FEMA hydrographs for the Snohomish River at a 10-year (Q_{10}), 50-year (Q_{50}) and 100-year (Q_{100}) return frequencies.

HOUR	Q_{10} Flows (cfs)	HOUR	Q_{50} Flows (cfs)	HOUR	Q_{100} Flows (cfs)
0	10,000	0	10,000	0	10,000
288	40,000	288	38,600	288	33,900
309	26,400	309	36,500	309	42,500
329	60,400	329	78,000	329	84,000
350	95,988	350	155,001	350	190,400
360	114,000	360	172,935	360	204,000
374	95,988	374	155,001	374	190,400
401	60,400	401	78,000	401	84,000
429	26,400	429	36,500	429	42,500
456	40,000	456	38,600	456	33,900
483	10,000	483	10,000	483	10,000
504	10,000	504	10,000	504	10,000

Table 5 – As in Table 4 but for the Pilchuck River.

HOUR	Q_{10} Flows (cfs)	HOUR	Q_{50} Flows (cfs)	HOUR	Q_{100} Flows (cfs)
0	800	0	800	0	800
313	800	313	800	308	800
319	1,000	319	1,000	320	1,000
331	1,700	331	1,700	332	1,650
343	3,300	343	3,300	344	3,400
355	6,800	355	8,800	350	5,900
357	7,250	357	9,700	358	10,900
359	7,500	359	10,000	360	11,000
361	7,400	361	9,800	362	10,900
367	6,000	367	8,000	368	8,800
373	4,700	373	6,200	380	5,450
379	3,650	379	5,000	392	3,600
391	2,450	391	3,400	404	2,550
403	1,900	403	2,500	416	1,750
427	1,400	427	1,750	428	1,300
439	1,200	439	1,400	452	850
451	1,000	451	1,200	476	800
487	800	487	800	487	800
504	800	504	800	504	800

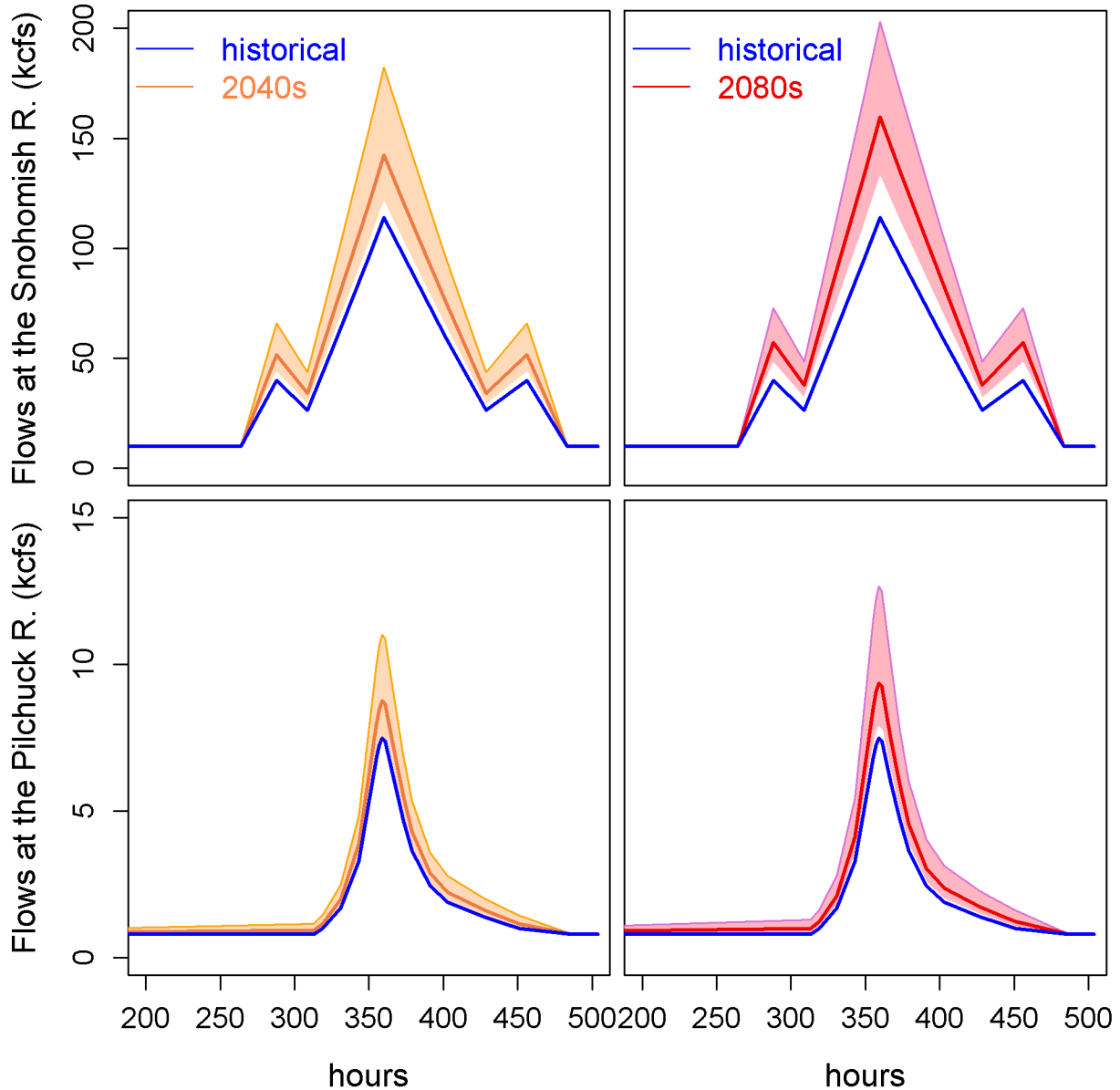


Figure 6 – Hydrographs of the 10-year (Q10) peak streamflow event for historical (blue) and scaled Q10 hydrograph for the 2040s (2030-2059; left panels) and 2080s (2070-2099; right panels), for the Snohomish River near Monroe (top panels) and the Pilchuck River (bottom panels). Changes are relative to 1970-1999, based on the moderate A1b greenhouse gas scenario. Orange and pink bands show the range associated with 10 statistically-downscaled GCMs. Solid orange and red lines show the average among all 10 models. Note the difference in scale between the top and bottom panels.

hydrographs by scaling these based on hydrologic model projections. The scaling factor was defined as the ratio of future to historical flood magnitude at 1-, 3-, 5- and 7-day consecutive highest flows for a return frequency of 10- (Q10) and 100-years (Q100; Tables 2 and 3). Future hydrographs were determined by applying the ratio to the historical hydrographs for a given return interval. For example:

$$\text{Future peak flow} = \text{observed historical peak flow} \times \frac{\text{simulated future flow}}{\text{simulated historical flow}}$$

This ratio was applied separately for each flow duration (1-, 3-, 5-, and 7-day) to obtain a modified synthetic hydrograph for each scenario. Figures 6 and 7 show the scaled hydrographs for the 2040s and 2080s alongside the historical hydrographs for each return period and streamflow input. These hydrographs were used as upstream boundary conditions in the HEC-RAS model.

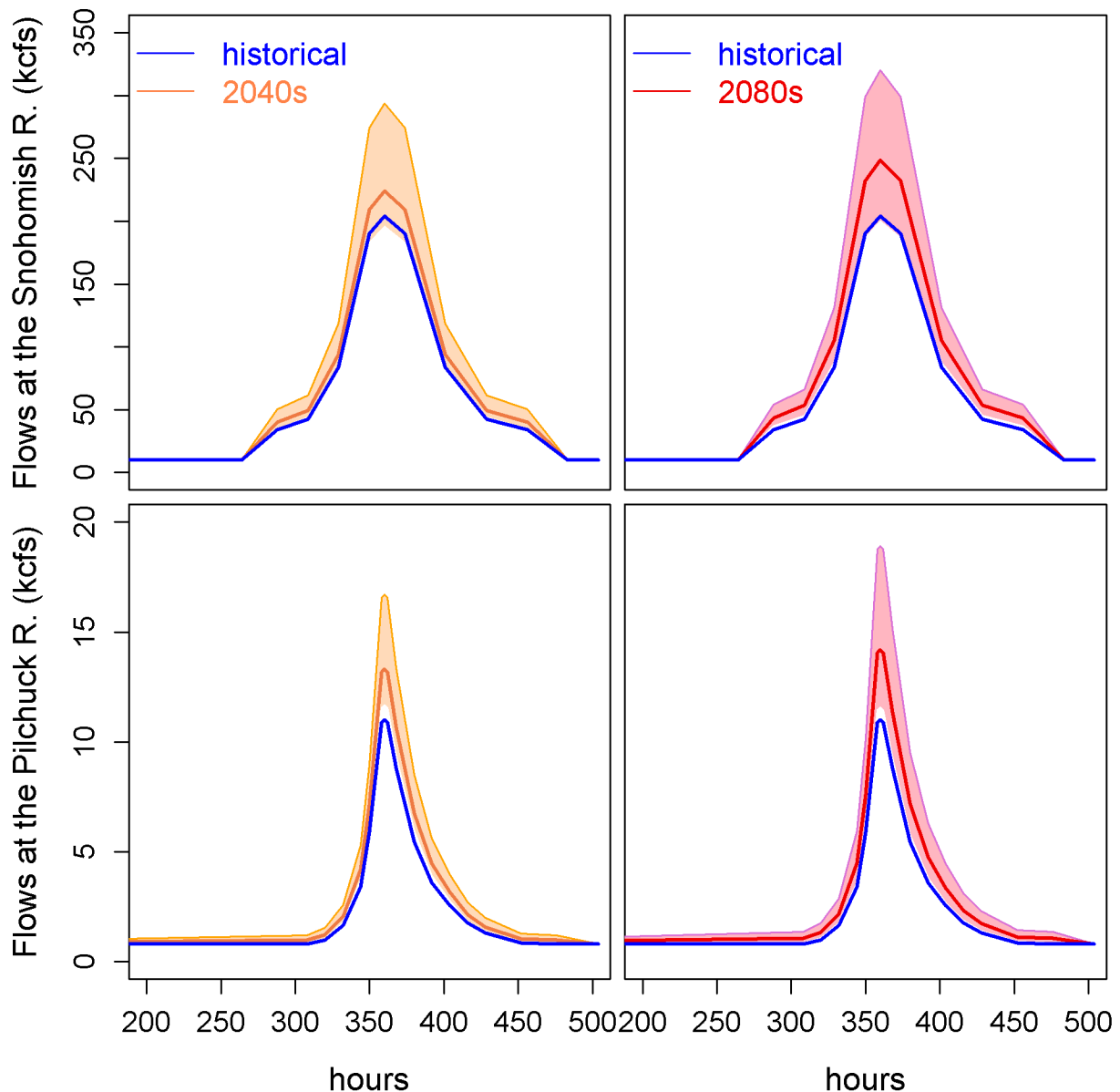


Figure 7 – As in Figure 6 but for the 100-year (Q100) event. Note that the y-axes are scaled differently than in the previous figure.

Lower Boundary Condition

The lower boundary condition to the model is determined by total water levels associated with sea level rise, tides, and surge, the latter a consequence of fluctuations in surface pressure, surface winds, and currents. Waves are not considered in the analysis – the Snohomish River delta is sheltered from large waves by Whidbey Island, and the HEC-RAS model does not simulate gravity waves.

Tides and Surge

Observed and predicted tides were obtained from NOAA (2014) for two Puget Sound stations, one at Everett near the mouth of the Snohomish River and another longer record from Seattle.

Since the two are independent, we separate astronomical tides from surge in the tidal analysis. We apply time-varying tides with a high-tide set to peak at mean high high water (MHHW) and coincide with peak flows in the Snohomish and Pilchuck Rivers. The WEST (2001) study cites a MHHW of 8.9 ft. (NAVD88, or 5.2 ft relative to NGVD). This value corresponds closely with NOAA (2014) values for nearby stations in Everett and Seattle. We used time-varying tides because simulations using constant tides, held constant at MHHW, showed slightly different results than those using the more realistic time-varying water levels.

Surge was estimated using “skew surge,” defined as the difference between the daily peak in observed and predicted tides (see e.g., McMillan et al., 2011). Simple tidal anomalies, based on hourly differences between observed and predicted tides, risk conflating differences in the phase (timing) with actual weather-driven surge events; skew surge is less susceptible to such errors.

The tide record at NOAA’s Seattle tide gauge is much longer than elsewhere in Puget Sound (hourly observations from 1901-present). Since the Seattle gauge is somewhat removed from the model boundary, we compared daily skew surge for the overlapping period between the two stations (04 Nov 1995 – 19 Feb 1996; about 3.5 months). The two records are highly correlated, with a squared correlation (r^2) of 0.98 (95% confidence limits, accounting for autocorrelation: 0.97-0.99). We therefore conclude that Seattle tides can serve as an accurate proxy for changes in surge at the mouth of the Snohomish River.

Using the most recent 50-years of hourly observations from Seattle, we obtain peak annual skew surge values for each year. These are fitted to a Generalized Extreme Value (GEV) distribution to estimate the 10-, 50-, and 100-year surge values (relative to MHHW) from the time series, using the same approach described above for peak flows (Table 6). Although extreme water levels are also available on the NOAA website, these are based on a 20-year record, which is likely inadequate for developing robust estimates of extreme values.

It is possible that climate change may affect extremes in surface pressure, winds, or circulations due to changes in storm frequency and strength. Hamman et al. (2012) evaluated this possibility, using regional climate model simulations (Salathé et al., 2010; Salathé et al., 2014) and a regression model trained on regional variations in sea level pressure and sea surface temperature associated with the El Niño Southern Oscillation (ENSO). Their results, based on a single global

model projection, suggest that climate change has very little influence on storm surge. This is consistent with the findings of Stammer and Hüttermann (2008).

Table 6 – Historical extreme surge values estimated from tidal observations in Seattle. Based on daily skew surge estimates (McMillan et al., 2011; see text), estimated using a Generalized Extreme Value (GEV) distribution. Values are relative to MHHW.

	10-yr (10% ACE)	50-yr (2% ACE)	100-yr (1% ACE)
Surge:	24 inches	30 inches	32 inches

Sea Level Rise

Sea Level Rise (SLR) projections were taken from the recent synthesis of projections for the West Coast by the National Research Council (NRC, 2012). Among projections of global sea level rise, the NRC projections are within the range of other recent projections – higher than the projections of the recent Intergovernmental Panel on Climate Change (IPCC, 2013) report, but lower than those of Vermeer and Rahmstorf (2009).

The hydrologic projections used in this study pertain to 30-year averages at mid- (2040s; 2030-2059) and late- (2080s; 2070-2099) century, relative to 1970-1999. In contrast, the SLR projections are for 2050 and 2100, relative to 2000. For consistency, the sea level projections were interpolated to 2045 and 2085, respectively, using a quadratic fit; the resulting values are shown in Table 7. Note that the baseline year (2000) is not the same as that used for the hydrologic projections. However, sea level in the northwest has remained fairly constant for the last 2 decades – the results are therefore similar to the change relative to 1970-1999.

Table 7 – Projections of *relative* sea level rise used in the analysis, including projected changes in both the absolute height of the sea surface (“Due to Sea Level Rise”), and the relative position of the land surface (“Due to Land Subsidence”). Projections were obtained from NRC (2012). SLR projections were interpolated to the 2040 and 2080 averages (2030-2059 and 2070-2099, respectively) using a quadratic fit. All changes are relative to the year 2000.

	Relative Sea Level Rise (inches)			
	<i>Due to Sea Level Rise</i>			<i>Due to Land Subsidence</i>
	<i>Low</i>	<i>Medium</i>	<i>High</i>	
2040s (2030-2059)	3.7	5.3	7.3	1.8
2080s (2070-2099)	9.8	16	22	3.3

Vertical Land Motion

In practice, sea level rise affects flooding via the combined effect of rising seas and vertical land motion. The Pacific Northwest is a tectonically active region, influenced by the subsiding Pacific plate and associated faults, earthquakes, and volcanoes; rebound since the retreat of ice age glaciers; sediment processes; and other factors that affect local rates of uplift/subsidence.

The Pacific Northwest Geodetic Array (PANGA, 2014) does not include sensors located specifically within the Snohomish River delta. Rates from nearby sensors range from -2 to -4 mm/yr (i.e.: subsidence), depending on location. In addition, parts of the floodplain appear to have experienced additional subsidence, possibly associated with increased drainage associated with agriculture. However, the PANGA observations require substantial post-processing to accurately estimate vertical rates – to date there are no such published estimates that are applicable to the lower Snohomish. As a conservative estimate, we instead used the published estimate from NRC (2012) for Anacortes, WA. That report estimates a subsidence rate of -1 mm/yr, corresponding to a decline in land elevation (and a corresponding rise in sea level, relative to land) of 4.5 cm for the 2040s and 8.5 cm for the 2080s.

Model runs

As described above, we used the HEC-RAS model to estimate the combined impacts of sea level rise, surge, and peak streamflow events on flooding. To do so requires consideration of the joint probability of peak surge and flow events, since areas that are influenced by both may expect to experience flooding more frequently. Since many of the drivers of heavy precipitation are also associated with surge, there is reason to expect that the two will be related, if somewhat lagged, relative to one another. We compared the daily time series of skew surge and streamflow and found that the two are essentially uncorrelated. Specifically, we found that the correlation was

Table 8 – Description of scenarios used to run hydrodynamic models.

Time Periods	Scenarios	Upstream Conditions	Downstream Conditions
Historical	Historical 100-yr Event (1% ACE)	Historical FEMA Q100 Hydrograph	Historical 100-yr Surge & No 10-yr
	Historical 10-yr Event (10% ACE)	Historical FEMA Q10 Hydrograph	Historical 10-yr Surge & No 10-yr
2080s	2080s high 100-yr Event (1% ACE)	2080s high Q100 hydrograph	Historical 100-yr Surge & 2080s high 10-yr
	2080s low 100-yr Event (1% ACE)	2080s low Q100 hydrograph	Historical 100-yr Surge & 2080s low 10-yr
	2080s high 10-yr Event (10% ACE)	2080s high Q10 hydrograph	Historical 10-yr Surge & 2080s high 10-yr
	2080s low 10-yr Event (10% ACE)	2080s low Q10 hydrograph	Historical 10-yr Surge & 2080s low 10-yr
2040s	2040s high 100-yr Event (1% ACE)	2040s high Q100 hydrograph	Historical 100-yr Surge & 2040s high 10-yr
	2040s low 100-yr Event (1% ACE)	2040s low Q100 hydrograph	Historical 100-yr Surge & 2040s low 10-yr
	2040s high 10-yr Event (10% ACE)	2040s high Q10 hydrograph	Historical 10-yr Surge & 2040s high 10-yr
	2040s low 10-yr Event (10% ACE)	2040s low Q10 hydrograph	Historical 10-yr Surge & 2040s low 10-yr

maximized at a lag of one day (peak surge occurring one day prior to peak flow), but still minuscule: an r^2 of 0.045 (95% confidence limits, accounting for autocorrelation: 0.035-0.055). This is convenient, since it means that we can consider peak surge and flow events to be statistically independent. As a result, we modeled the upstream (peak flow) and downstream (SLR, surge) events separately, and then took the maximum water surface elevation among the two simulations to make inundation maps.

Flood simulations (Table 8) were performed for both the 10- and 100-year floods, for the historical (1970-1999) and two future time periods (2040s, 2080s). Each future time period was modeled using two scenarios: one showing the smallest change (“low”), and the other showing the greatest change (“high”) relative to the historical period. In all, a total of 10 hydraulic simulations were performed.

Results

Figures 8 and 9 show simple GIS maps that highlight the extent of the 10-year and 100-year floods for the historical and future (2080s) simulations. Created in order to emphasize changes in the area inundated, the shaded areas highlight any area with a non-zero water depth. It is immediately apparent that projected changes in the areal extent of flooding are large for the 10-year flood, but quite small for the 100-year flood. This is not surprising, since the levees in the lower basin are primarily 10-year levees. This means that the historical 100-year flood, under present-day conditions, should already result in flooding that extends from valley wall to valley wall, with generally small changes going into the future. In contrast, small changes in the volume of the 10-year flood may lead to large changes in the area inundated. As a result, we expect the primary change in area inundated to be an increase in the frequency of moderate flood events rather than a change to the most extreme events.

Results from this study were incorporated into TNC’s “coastalresilience” (CR) decision support tool, which allows users to interactively explore the study results, along with numerous other spatial datasets. Figures 10 and 11 show screenshots of inundation maps as they are displayed in the CR tool. In contrast with Figures 8 and 9, these maps include both changes in depth and area. Changes in the depth of inundation, in contrast to areal extent alone, are notable for all scenarios.

Both sets of maps highlight the large range among projected changes – the high and low scenarios represent very different changes in flood risk. It is possible that some of the range in projections may be reduced with improved models – indeed, global climate models are increasing in sophistication, and we will likely soon be able to consider a dynamically downscaled (i.e., using a regional climate model) ensemble of projections as opposed to simply statistically downscaled projections. Although these will add important detail, a substantial proportion of the uncertainty in these projections is likely irreducible, for two reasons: (1) Random natural variability will continue to result in unpredictable variations in climate, and (2) We cannot predict the future: 21st century human emissions of greenhouse gases are dependent on a variety of factors (population, technology, geopolitics, etc.) that are difficult to foretell with any accuracy. However, this does not preclude planning in response to climate change – as discussed by Snover et al. (2013), planning decisions are almost always based on uncertain information. In this study we have included a low and a high projection for each time period as

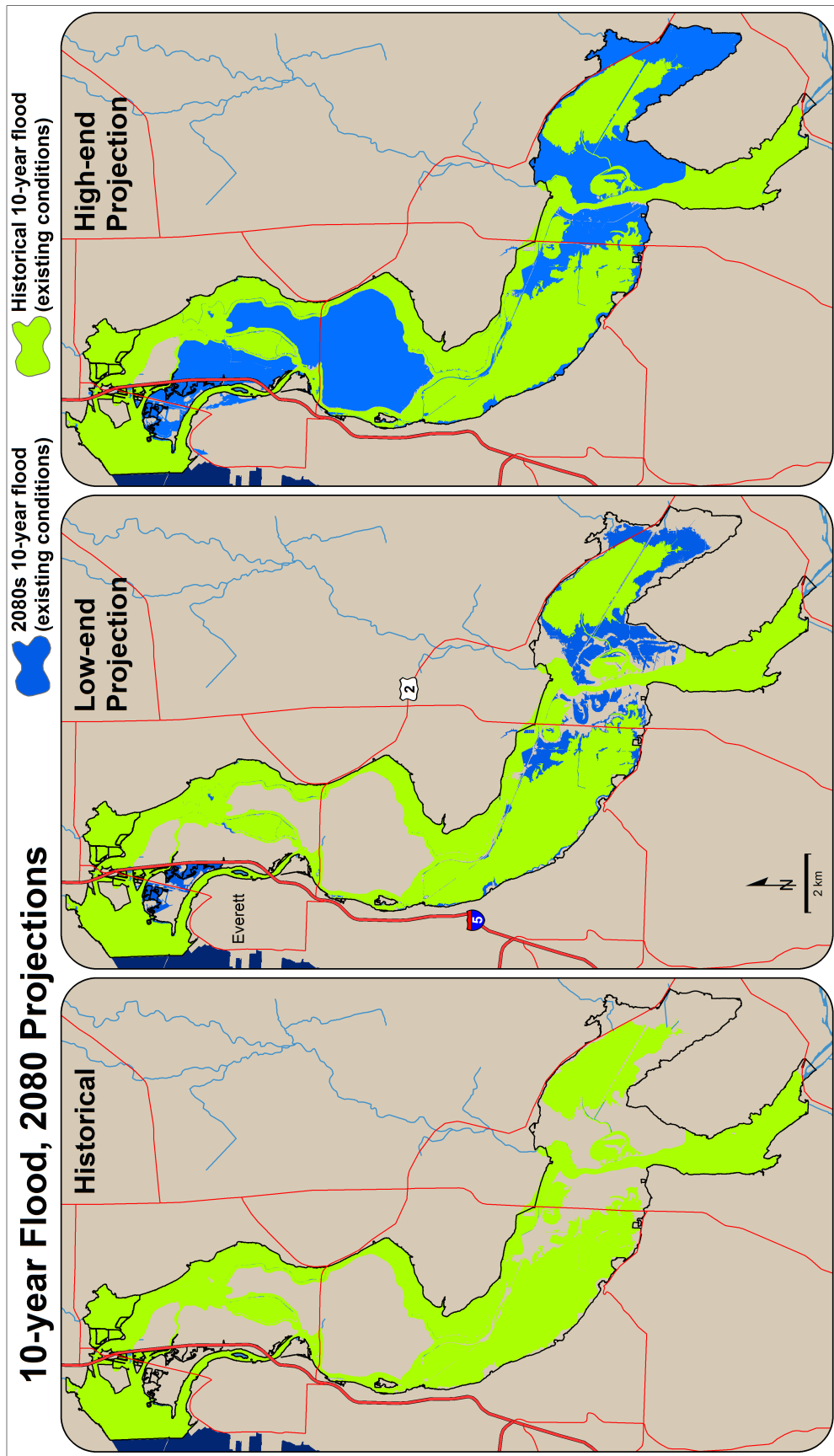


Figure 8 – Areal extent of historical (green) and future inundation (blue) for the 10-year flood (10% ACE). Historical inundation is shown in all 3 panels, and alone in the left panel. Future projections are for the 2080s (relative to 1970-1999, A1b scenario), showing a low- (middle panel) and a high-end (right panel) projection.

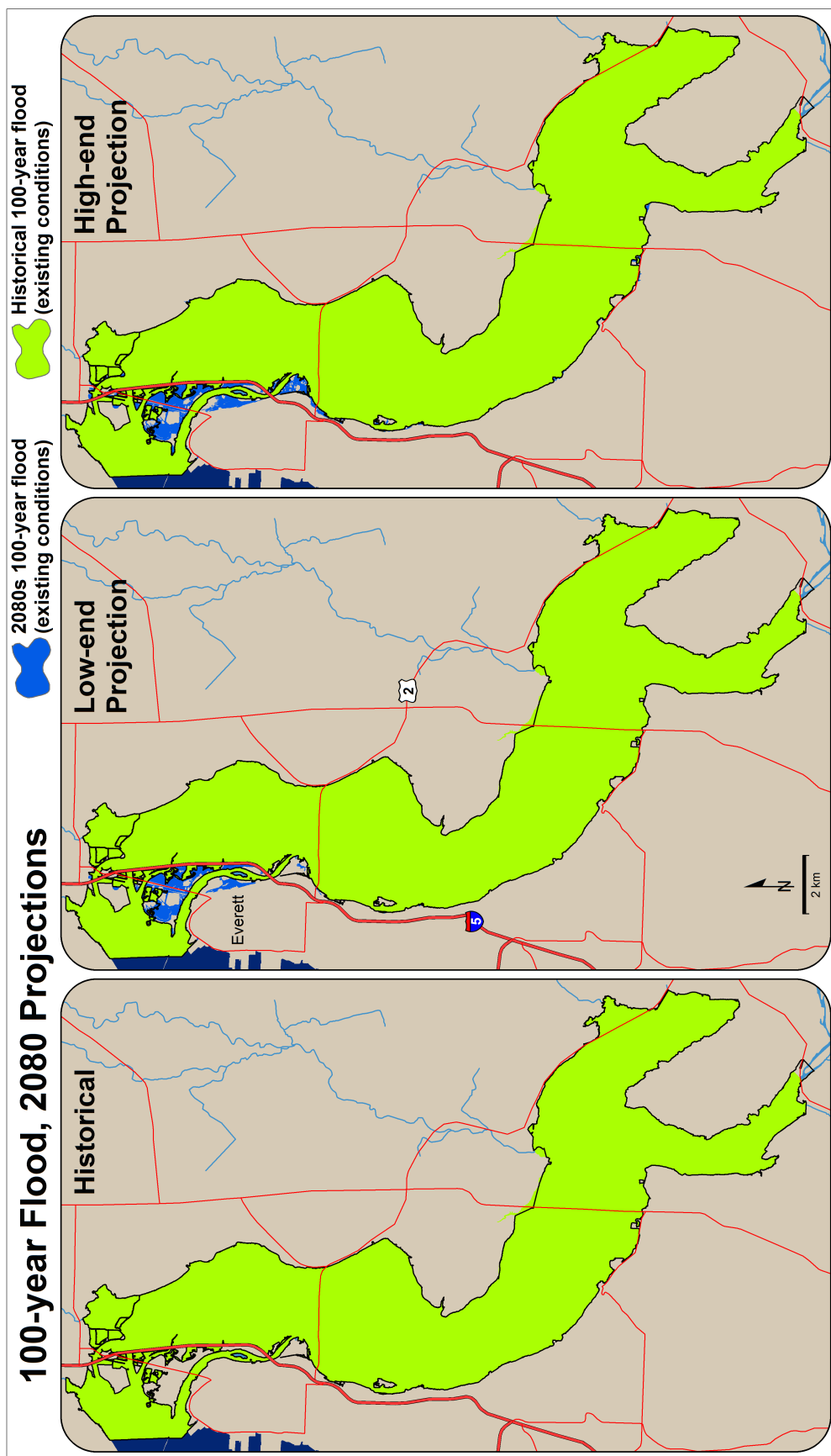


Figure 9 – As in Figure 8 but for the 100-year flood.

the basis for adaptation decisions. Some planning decisions, especially those with a long time horizon, will need to be robust to the worst case scenario – in these cases it will be appropriate to focus on the high scenario. Other planning contexts may be more iterative approach, in which plans are adaptive over time – these may be best suited to considering the full range among scenarios.

We also evaluated the relative importance of sea level rise and peak river flows. We found that flood events are primarily driven by peak river flows upstream of the Ebey-Steamboat connector and primarily driven by surge and sea level rise downstream of that point. Note that surge events can influence water elevations much farther upstream than this point, and that the converse is true for streamflow – the Ebey-Steamboat connector is simply the point above which the 10- or 100-year peak river flow event results in much higher water levels than for the corresponding surge event.

As a final set of simulations we also evaluated the impact of levee modifications. In consultation with staff at Snohomish County, we identified two alternative levee scenarios which we could model. The first involved removing the levees protecting Crabb and Beck dikes, which are near the upstream end of the model domain. The second alternative involved breaching the levees protecting Spencer Island, so that it could serve as a storage area for excess flood volume. We do not present maps of the results of these simulations because neither had an appreciable effect on flooding. In the case of Crabb and Beck dikes, the storage areas were simply too small to have any effect – too small even to substantially lower water levels in the immediate vicinity of the dikes. The Spencer Island modification was similarly ineffectual, but primarily because of the low elevation of the island – Spencer Island is frequently flooded by salt water, thus leaving little extra storage area for freshwater flows. Although there are other options for providing flood storage, few are currently viable as options given current floodplain development and interests.

Finally, we note that one goal of this study was to provide a proof-of-concept for incorporating climate change into flood risk assessment and planning. By using a hydraulic model that was essentially off-the-shelf, we were able to assess the combined impacts of SLR and streamflow on flooding at a relatively low cost. Having now established the methodology, this approach could be applied elsewhere in the region at a much lower cost than for the present proposal. In addition, we note that this study focused on just two pathways for climate change impacts on floodplains: sea level rise and changing peak river flows. These are key factors, but there are other mechanisms by which climate may impact flood risk (e.g.: wildfires, sediment transport, landslides), in addition climate change impacts extend beyond changes in flood risk (e.g.: riparian habitat, groundwater, saltwater intrusion, water temperature). More work is needed to evaluate these risks and determine their relevance to managers, tribes, agriculture, and other key stakeholders.

Acknowledgements

The authors would like to thank The Nature Conservancy (TNC), which provided funding for the work, and Kris Johnson at TNC for developing the original idea. We would also like to thank Ray Walton and Sarah Bengston at WEST consultants for their work developing and post-processing the hydraulic model output.

10-year Flood, 2080 projections

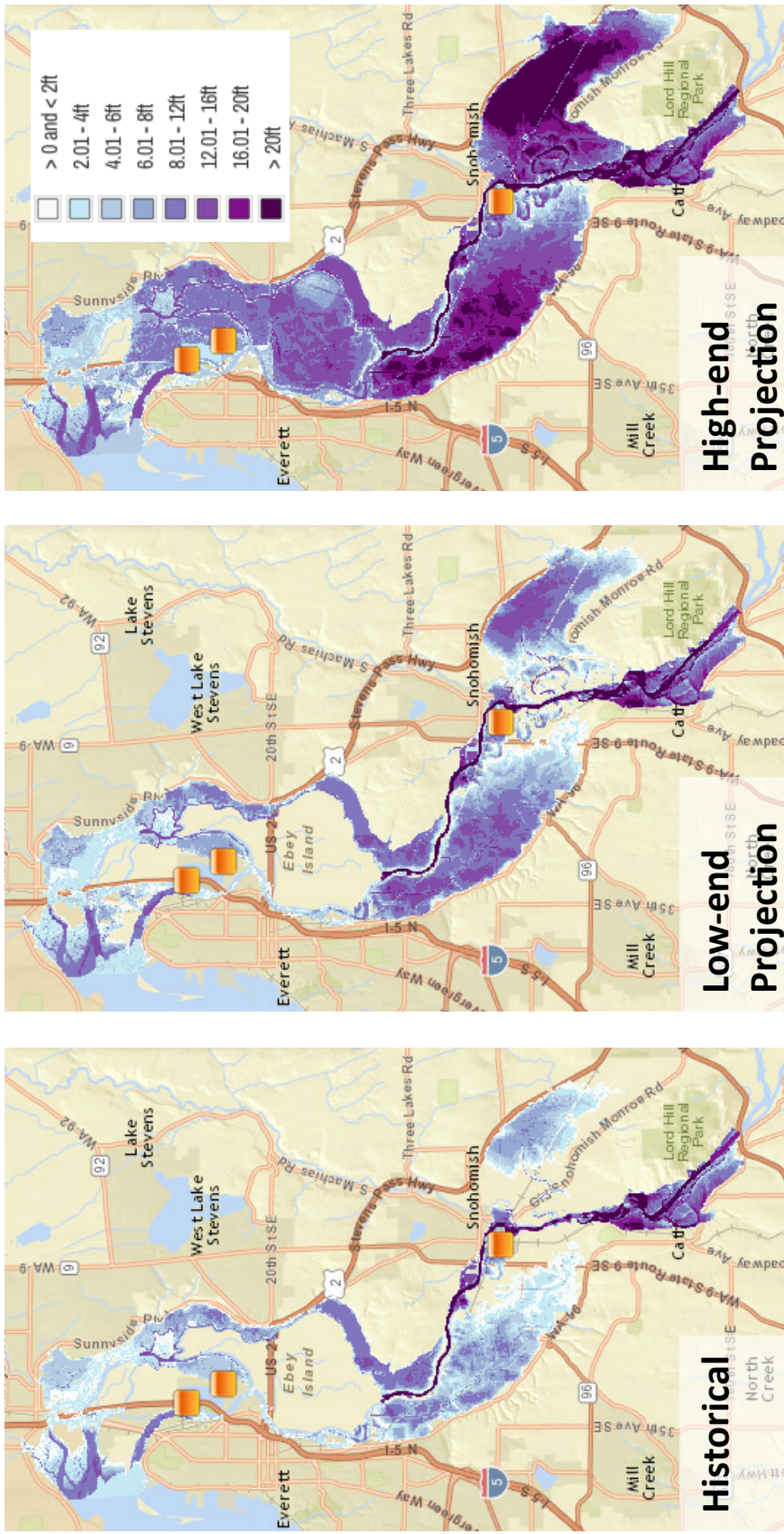


Figure 10 – Screenshots from the “CoastalResilience” (CR) tool showing the area and extent of inundation for the 10-year flood. Maps show historical (left panel) and two future projections for the 2080s, A1b scenario (relative to 1970-1999): a low- (middle panel) and high-end (right panel) projection.

100-year Flood, 2080 projections

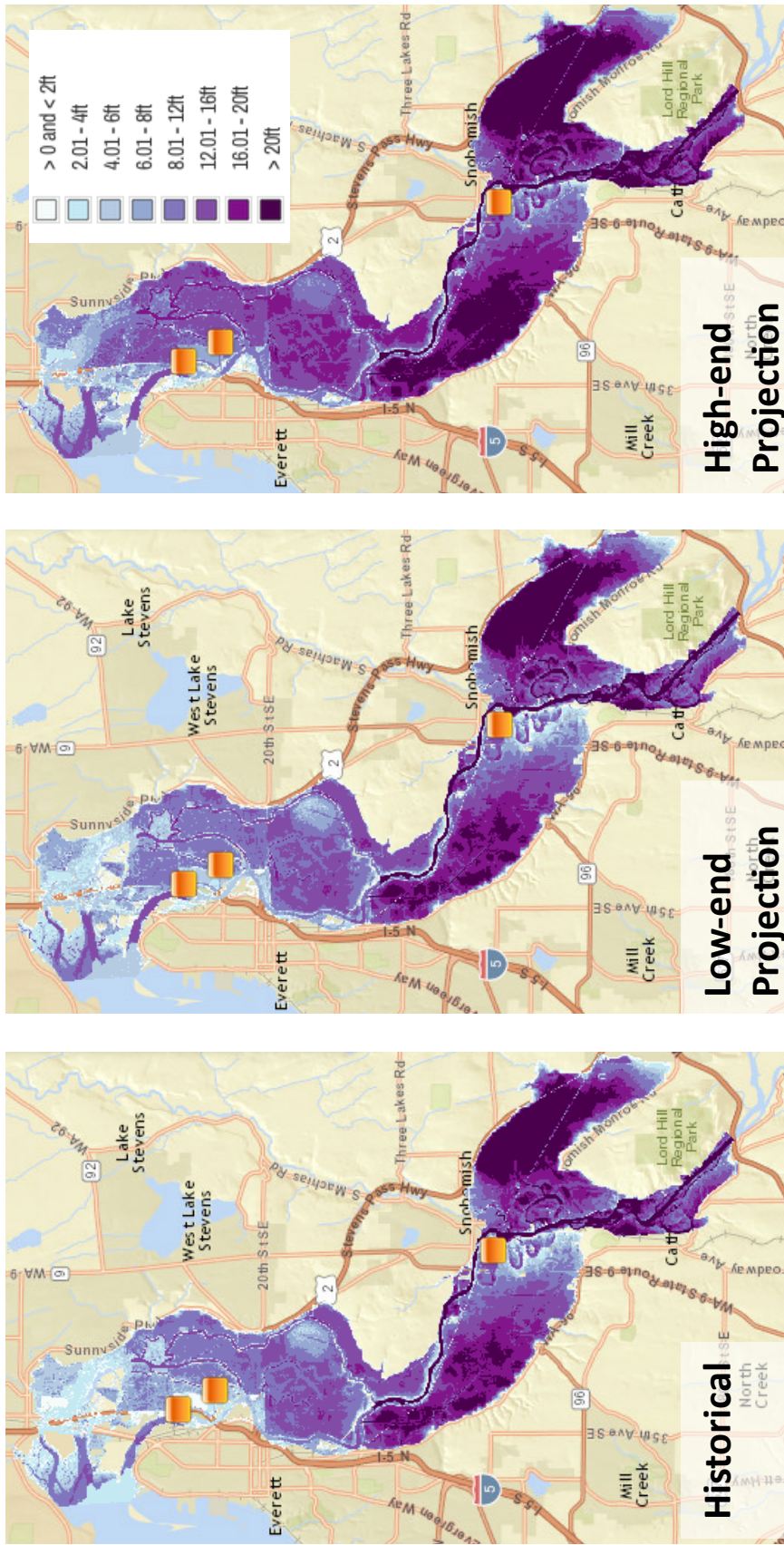


Figure 11 – As in Figure 10 but for the 100-year flood.

References

- Abatzoglou, J. T., & Brown, T. J. (2012). A comparison of statistical downscaling methods suited for wildfire applications. *International Journal of Climatology*, 32(5), 772-780.
- Elsner, M. M., Cuo, L., Voisin, N., Deems, J. S., Hamlet, A. F., Vano, J. A., Mickelson, K. E. B., Lee, S.-Y., and Lettenmaier, D. P. (2010). Implications of 21st century climate change for the hydrology of Washington State. *Climatic Change*, 102(1-2), 225-260.
- Gao, H., Tang, Q., Shi, X., Zhu, C., Bohn, T. J., Su, F., Sheffield, J., Pan, M., Lettenmaier, D. P., and Wood, E. F. (2010). Water budget record from Variable Infiltration Capacity (VIC) model. *Algorithm Theoretical Basis Document for Terrestrial Water Cycle Data Records*.
- Hamlet, A.F., Elsner, M.M. Mauger, G., Lee, S-Y, and Tohver, I. (2013). An Overview of the Columbia Basin Climate Change Scenarios Project: Approach, Methods, and Summary of Key Results, *Atmosphere-Ocean*, 51:392-415.
- Hamman, J.J., Hamlet, A.F., Grossman, E.E., Fuller, R. (2014). Effects of Projected Twenty-First Century Sea Level Rise, Storm Surge, and River Flooding on Water Levels in the Skagit River Floodplain. *Manuscript in preparation*.
- Hamman, J. J. (2012). Effects of Projected Twenty-First Century 10-yr, Storm Surge, and River Flooding on Water Levels in Puget Sound Floodplains and Estuaries (Master's Thesis, University of Washington). <http://hdl.handle.net/1773/20735>
- Hosking JRM, Wallis JR, 1993. Some statistics useful in regional frequency analysis, *Water Resources Research*, 29(2):271-281.
- Intergovernmental Panel on Climate Change (IPCC), (2013). Working Group 1, Summary for Policymakers. Available at:
http://www.climatechange2013.org/images/uploads/WGIAR5-SPM_Approved27Sep2013.pdf
- Liang X, Lettenmaier DP, Wood EF, Burges SJ. (1994). A simple hydrologically based model of land surface water and energy fluxes for GSMS. *Journal of Geophysical Research*, 99, 14,415–14,428.
- Lohmann, D., Nolte-Holube, R. and Raschke, E., (1996) A large scale horizontal routing model to be coupled to land surface parameterization schemes. *Tellus* 48 A, pp. 708–72
- McMillan, A., Batstone, C., Worth, D., Tawn, J., Horsburgh, K., & Lawless, M. (2011). Coastal flood boundary conditions for UK mainland and islands. Project SC060064/TR2: Design sea levels.
- Meehl, G. A., Covey, C., Taylor, K. E., Delworth, T., Stouffer, R. J., Latif, M., McAvaney, B. and Mitchell, J. F. (2007). The WCRP CMIP3 multimodel dataset: A new era in climate change research. *Bulletin of the American Meteorological Society*, 88(9), 1383-1394.
- Nakicenovic, N. et al., 2000. Special Report on Emissions Scenarios: A Special Report of Working Group III of the Intergovernmental Panel on Climate Change, Cambridge University Press, Cambridge, U.K., 599 pp. Available online at:
<http://www.grida.no/climate/ipcc/emission/index.htm>
- National Oceanic and Atmospheric Administration (NOAA), Tides and Currents (2014). Observed and predicted hourly water levels for Seattle (9447130) and Everett (9447659) stations. Retreived from <http://tidesandcurrents.noaa.gov/> on 8 April 2014.

- National Research Council. Sea-Level Rise for the Coasts of California, Oregon, and Washington: Past, Present, and Future. Washington, DC: The National Academies Press, 2012.
- Pacific Northwest Geodetic Array (PANGA) (2014). Retrieved from <http://www.panga.org/> on 30 May 2014.
- Roeckner, E., L. Bengtsson, J. Feichter, J. Lelieveld, and H. Rodhe (1999): Transient climate change simulations with a coupled atmosphere-ocean GCM including the tropospheric sulfur cycle. *J. Climate*, 12, 3004-3032.
- Roeckner, E. et al. (2003): The atmospheric general circulation model ECHAM5, Part I: Model description, Max-Planck-Institute for Meteorology Report No. 349.
- Salathé, E. P. Jr., Hamlet, A. F., Mass, C. F., Lee, S.-Y., Stumbaugh, M., and Steed, R., (2014). Estimates of Twenty-First-Century Flood Risk in the Pacific Northwest Based on Regional Climate Model Simulations. *J. Hydrometeor.*, 15, 1881–1899. doi: <http://dx.doi.org/10.1175/JHM-D-13-0137.1>
- Salatthe Jr, E. P., Leung, L. R., Qian, Y., & Zhang, Y. (2010). Regional climate model projections for the State of Washington. *Climatic Change*, 102(1-2), 51-75. doi: 10.1007/s10584-010-9849-y
- Snover, A. K., Mantua, N. J., Littell, J. S., Alexander, M. A., McClure, M. M., & Nye, J. (2013). Choosing and Using Climate-Change Scenarios for Ecological-Impact Assessments and Conservation Decisions. *Conservation Biology*, 27(6), 1147-1157.
- Snover, A.K., Hamlet, A.F., and Lettenmaier, D.P. (2003). Climate-change scenarios for water planning studies: Pilot applications in the Pacific Northwest. *Bulletin of the American Meteorological Society*, 84 (11), 1513-1518.
- Stammer, D., & Hüttemann, S. (2008). Response of regional sea level to atmospheric pressure loading in a climate change scenario. *Journal of Climate*, 21(10), 2093-2101. doi:10.1175/2007JCLI1803.1
- Stedinger, J. R., Vogel, R. M., and Foufoula-Georgiou, E., (1993). Frequency analysis of extreme events. *Handbook of Hydrology*, D. R. Maidment, ed., McGraw-Hill, Inc, New York.
- Tohver, I. M., Hamlet, A. F. and Lee, S.-Y., (2014). Impacts of 21st-Century Climate Change on Hydrologic Extremes in the Pacific Northwest Region of North America. *Journal of the American Water Resources Association (JAWRA)*. 50(6):1461-1476. DOI: 10.1111/jawr.12199
- Vano, J. A., Voisin, N., Cuo, L., Hamlet, A. F., Elsner, M. M., Palmer, R. N., Polebitski, A., and Lettenmaier, D. P. (2010). Climate change impacts on water management in the Puget Sound region, Washington State, USA. *Climatic Change*, 102(1-2), 261-286.
- Vermeer, M., & Rahmstorf, S. (2009). Global sea level linked to global temperature. *Proceedings of the National Academy of Sciences*, 106(51), 21527-21532.
- Wang Q. J., (1997). LH moments for statistical analysis of extreme events. *Water Resources Research*, 33(12):2841-2848.
- WEST Consultants, Inc. (WEST), (2012). Everett Riverfront Development 90% and 60% Hydraulic Analysis, memo prepared to MacLeod-Reckord, Inc, Seattle, Washington, May 1, 2012.
- WEST Consultants, Inc. (WEST), (2011). Hydraulic Analysis for Smith Island Restoration, Appendix A in *Geomorphic Characterization and Channel Response Assessment for*

Union Slough, prepared by GeoEngineers, Seattle, Washington, for Snohomish County Surface Water Management Division, May 31, 2011.

WEST Consultants, Inc. (WEST), (2001). Technical Support Data Notebook for Snohomish County, City of Everett, City of Marysville, City of Snohomish, and Unincorporated Areas, Restudy Flood Insurance Study, prepared for Seattle District, Corps of Engineers, and FEMA Region 10, April 2001.